Available online at www.sciencedirect.com
SCIENCE DIRECT
Polymer 46 (2005) 9840–9850
polymer
www.elsevier.com/locate/polymer

Improving the adhesion of poly(ethylene terephthalate) fibers to poly(hydroxyethyl methacrylate) hydrogels by ozone treatment: Surface characterization and pull-out tests

Lino Ferreira[a,*], Marta B. Evangelista[a], M[a] Cristina L. Martins[a], Pedro L. Granja[a], José L. Esteves[b], Mário A. Barbosa[a,c]

[a]*INEB-Instituto de Engenharia Biomédica, Laboratório de Biomateriais, Rua do Campo Alegre, 823, 4150-180 Porto, Portugal*
[b]*Universidade do Porto, Faculdade de Engenharia, Departamento de Engenharia Mecânica, Porto, Portugal*
[c]*Universidade do Porto, Faculdade de Engenharia, Departamento de Engenharia Metalúrgica e de Materiais, Porto, Portugal*

Received 7 October 2004; received in revised form 3 July 2005; accepted 9 August 2005
Available online 31 August 2005

Abstract

This work reports a methodology to improve the adhesion between poly(ethylene terephthalate) (PET) fibers and poly(hydroxyethyl methacrylate) (pHEMA) hydrogels by treating PET with ozone. The surface chemistry of PET was examined by water contact angle measurements, X-ray photoelectron spectroscopy (XPS), infrared reflection absorption spectroscopy (IRAS) and attenuated total reflectance infrared spectroscopy (ATR-IR) yielding information about the chemical functionalities at depths upon 0.6 μm. Ozone treatment introduces several polar groups in the surface of PET through oxidation and chain scission resulting in increased wettability. These groups include mostly carboxylic and anhydride groups and in small extent hydroxyl groups. Atomic force microscopy (AFM) analysis shows that the surface of ozone-treated PET films is fully covered with spherical particles that are removed after washing the film with water. During the washing step carboxylic functionalities were removed preferentially, as demonstrated by XPS and IR analysis. According to pull-out tests, PET monofilaments and bundles treated by ozone had a higher adhesion to pHEMA hydrogels than untreated ones. The apparent interfacial shear strength is 65% higher on pHEMA hydrogel containing an ozonated than an untreated PET monofilament. In addition, the force to pull-out an ozone-treated PET bundle from pHEMA hydrogel is ca. 81% higher than the one observed for the untreated bundle.

Keywords: Poly(ethylene terephthalate); Surface characterization; Pull-out tests

1. Introduction

The degeneration of the intervertebral disc is the main cause of low back pain. It is estimated that low back pain accounts for the fifth most common reason for time lost from work and physician office visits, just after the common cold [1]. Several devices have been proposed to substitute part or the whole disc [2,3]; however, most of them are still looking for FDA/CE approval and are still in clinical trial [2].

In the present work, in order to design an alternative intervertebral disc prosthesis with appropriate transport, mechanical and biological properties, a poly(2-hydroxyethyl methacrylate) (pHEMA) hydrogel based matrix, reinforced with poly(ethylene terephthalate) (PET) fibers was prepared. However, PET fibers exhibit low surface energy resulting in poor wettability and weak adhesion to pHEMA hydrogel matrix and this may reduce the mechanical performance of the overall disc substitute. In order to improve the interfacial bonding between PET fibers and pHEMA hydrogels the fiber surface needs to be modified. PET surface modification can be accomplished either through gas-phase techniques including plasma [4,5], corona discharge [4,6], flame treatment [4], UV/ozone [4,7,8], UV [9,10] and ozone only [4,7], or wet chemistry including aminolysis [11], hydrolysis [12], reduction [12],

* Corresponding author. Tel.: +351 226074900; fax: +351 226094567.
E-mail addresses: lino@mit.edu, lsf@ined.up.pt (L. Ferreira).

0032-3861/$ - see front matter © 2005 Elsevier Ltd. All rights reserved.
doi:10.1016/j.polymer.2005.08.033

activation of alcohol chain ends with tosyl chloride and subsequent chemistry [13], graft copolymerisation of vinyl compounds by chemical initiation [14], ion beam treatment in the presence of vinyl monomers [15], among others. In some cases, the chemical surface modification of PET requires the use of strong catalysts (e.g. reduction; grafting copolymerisation; tosyl chloride activation) and reagents (e.g. aminolysis), and special care needs to be taken in order to eliminate these substances after reaction. Therefore, this strategy is less appropriate considering the final in vivo application of the pHEMA/PET fiber discs.

From the main gas-phase techniques for modifying PET fibers, ozone has particular advantages due to the simplicity of the technique and its low-cost. This technique does not require high vacuum technology and is suitable for the modification of 3D objects, albeit requiring much more time to reach the same levels of oxidation as other gas-phase techniques [4]. However, it has been reported that the ageing process on ozone-treated films is slower than the one observed with other treatments [8]. Unfortunately, despite the published data, not enough information is available regarding the surface chemistry on ozone-treated PET. This information is important to evaluate the adhesion and stabilization of ozone-treated PET with different matrixes. Furthermore, the adhesion between ozone-treated PET fibers and hydrogel matrixes has not been reported and this is of primordial importance for their ultimate application in the design of intervertebral disc substitutes. In fact few studies have reported the adhesion of fibers to hydrogels [16].

In this work, PET fibers/films were treated by ozone for different times and their surface chemistry and morphology characterized. After ozone-treatment several polar groups were observed in the surface of PET, mostly carboxylic and anhydride groups and in small extent hydroxyl groups. According to pull-out tests, PET monofilaments and bundles treated by ozone had a higher adhesion to pHEMA hydrogels than untreated ones.

2. Experimental

2.1. Materials

PET films (thickness of 56 μm) and bundles (containing 247 PET monofilaments, each one with an average diameter of 25 μm) were kindly provided by Prof Luigi Ambrosio from Interdisciplinary Research Center in Biomedical Materials at University of Naples. PET films were used for contact angle measurements, XPS, AFM and ATR-IR analysis while PET bundles and monofilaments were used in pull-out tests (see below). In both cases, the T_g and M_n were 79.4–80.2 °C and 34,590 Da ($M_w/M_n = 1.8$), respectively. 2-Hydroxyethyl methacrylate (HEMA) and ethylene glycol dimethacrylate (EGDMA) were purchased from Aldrich while 2,2-azobisisobutyronitrile (AIBN) was obtained from Fluka.

2.2. Spin coating

PET was dissolved in trifluoroacetic acid (TFA) to an initial concentration of 1.8% (w/w) and several dilutions were prepared. A volume of 15 μL of the polymer-containing solution was dropped on silicon plates ($1\times 1\ cm^2$) with a sputtered chromium and gold layer (these plates are further referred as gold plates), and the plates were rotated at 2000 rpm for 1 min in a spin coater (model G3P-8, from Specialty Coating Systems, Inc.).

2.3. Ellipsometry

Ellipsometry measurements were performed using an imaging ellipsometer (model EP^3, from nanofilm surface analysis). The ellipsometer is an optical instrument that measures the changes in the polarization of light due to reflection and was operated in a polarizer–compensator–sample–analyzer (PCSA) mode (null ellipsometry). The light source was a solid-state laser with a wavelength of 532 nm. The gold plate refractive index (n) and extinction coefficient (k) were determined by using a delta and psi spectrum with a variation of angle between 60 and 75°. These measurements were made in four zones to correct for any instrument misalignment. To determine the thickness of the PET film deposited into the gold plate, the same kind of spectrum was used and n and k for the polymeric layer were set as 1.64 [17] and zero, respectively.

2.4. Ozone treatment

PET films ($10\times 20\ cm^2$) and fibers mounted into a stainless steel support, were treated with ozone (O_3) gas in a sealed cylindrical ($Ø = 36$, length = 35.8 cm) stainless steel reactor. The ozone was generated by a Fischer Ozone 502 apparatus that was coupled to an oxygen supplier (Medical Grade, Gasin, Portugal) at a flow rate of 400 L O_2 per hour. In these conditions, ozone is formed at a concentration of 0.078 mmol L^{-1}, as determined by iodometric–thiosulfate titration. Samples were treated for up to 6 h. In some cases, samples were washed with deionized water for 10 min and dried in a vacuum oven for 18 h, at 25 °C.

2.5. AFM analysis

AFM images were obtained in the Tapping mode, in air, with a AFM Pico Plus apparatus (molecular imaging). Microfabricated bar-shaped silicon cantilevers (NCH type from Scientec) with a theoretical spring constant of 25–50 N/m and resonance frequency of 263.9 kHz were used. The image processing and roughness analysis were performed with the 'scanning probe image processor (SPIP™)' (image metrology). The roughness average (S_a)

and root mean square (S_q) for a certain scanned area ($N \times N$) were calculated according to Eqs. (1) and (2), respectively:

$$S_a = \sum_{x,y=1}^{N} \frac{(Z_{x,y} - Z_{average})}{N^2} \quad (1)$$

$$S_q = \sqrt{\sum_{x,y=1}^{N} \frac{(Z_{x,y} - Z_{average})^2}{N^2}} \quad (2)$$

where $Z_{x,y}$ are the local heights, $Z_{average}$ is the average height determined over all x, y coordinates (N) measured in the AFM image. Before each roughness calculation the original image was treated with a least mean square average profile (third degree).

2.6. XPS analysis

XPS measurements were carried out on a VG Scientific ESCALAB 200A (UK) spectrometer using Al K_α (1486.6 eV) radiation source (15 kV, 300 W). The operating pressure during analysis was in the low 10^{-9} Torr range. Survey spectra were collected over a range of 0–1100 eV with analyser pass energy of 50 eV. High-resolution C(1 s) and O(1 s) spectra were collected with an analyser pass energy of 20 eV. In both cases, 10 mm^2 of the sample was examined and the atomic compositions were quantified using tabulated sensitivity factors. The spectra were fitted by a Lorentzian–Gaussian function, using a XPS peak-fitting program (XPSPEAK Version 4.1). The charging correction was made according to the aromatic carbon using the binding energy of 284.60 eV [5]. Angle-resolved analysis was also used for depth profiling the treated PET film. The sampling depth (d) is limited by the inelastic mean free path (λ) of the photoelectrons, according to the equation [5]:

$$d = 3\lambda \sin\theta \quad (3)$$

A value of 2.7 nm [18] was assumed for λ of the C1 s photoelectrons in PET.

Labelling reactions for hydroxyl and carboxyl groups were used to determine the concentration of these functional groups by XPS. The methodology adopted was reported elsewhere [12] and consisted in two steps: first, the labelling of hydroxyl groups by heptafluorobutyryl chloride followed by the labelling of carboxyl groups by 1,1′-carbonyldiimidazole.

2.7. Contact angle measurements

Contact angle measurements were performed using the sessile drop method with a contact angle measuring system from Data Physics (model OCA 15) equipped with a video CCD-camera and SCA 20 software. Untreated or ozone-treated PET films (2×2 cm^2) were placed in a closed, thermostated chamber (25 °C) saturated with water in order to prevent its evaporation. Static contact angles were measured by placing a water droplet (3 μL) onto the sample surface with an electronically regulated syringe. The angle was measured after 1 min of water contact with the sample. Subsequently, the water droplet was slowly increased or decreased in volume in order to obtain the advancing or receding water contact angles, respectively. Every contact angle was determined at four different spots on the sample. In the contact angle measurements of ozone-treated PET the dissolution of oxidized material in the probe liquid is likely to occur [7,8,19] and, therefore, may alter the surface energy. Despite this problem, contact angle measurements still yield a semi-quantitative measure of the wettability of the surface-treated PET in agreement with previous studies [7,8,19].

2.8. ATR-IR and IRAS analysis

ATR-IR and IRAS measurements were performed on a spectrophotometer (Perkin–Elmer, model 2000) coupled with an ATR (split-pea) or IRAS accessories and a nitrogen-cooled mercury cadmium telluride (MCT) detector. One hundred scans were performed with a resolution of 4 cm^{-1}. In ATR-IR measurements, the penetration depth (DP) of the radiation within the PET film was calculated according to Harrick equation [20]:

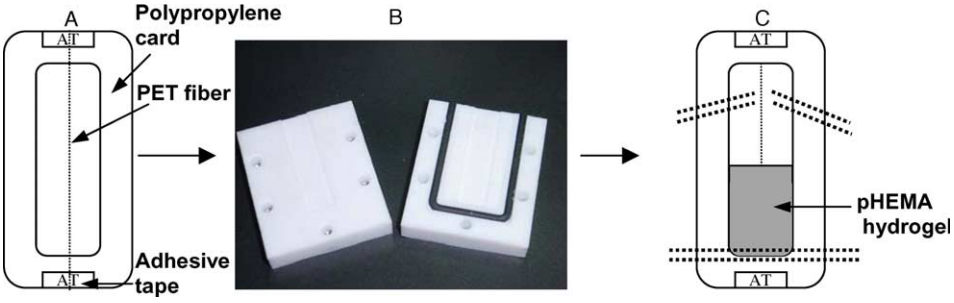

Fig. 1. Preparation of pHEMA hydrogels reinforced with PET fibers used for pull-out tests. (A) PET fiber attached to polypropylene card, (B) PTFE moulds used for HEMA polymerisation and (C) final material comprising PET fiber and pHEMA hydrogel (dotted lines represent the places, where propylene cards were sliced before the evaluation by pull-out tests).

$$DP = \frac{1}{2\pi\nu N_c(\sin^2\theta - N_{sc}^2)^{1/2}} \quad (4)$$

where ν is the wavenumber (cm^{-1}), N_c is the refraction index of the crystal (silicon, 3.42), θ is the incidence angle of the infrared radiation into the crystal (45°), N_{sc} is the ratio between the refraction index of PET sample (1.64) and the crystal. In IRAS measurements a silicon plate covered with gold was used as background. PET deposited on gold plates by spin coating (see above) and treated by ozone for different times were used as samples. The deconvolution of the spectra was performed by PeakFit software (version 4.11, Systat, Inc.) from the apparatus.

2.9. SEM analysis

Samples were either carbon or gold coated by sputtering (JEOL JFC 1100) and then examined with a JEOL JSM-6301F scanning electron microscope using an accelerating voltage of 15 kV.

2.10. Pull-out tests of pHEMA hydrogels reinforced with untreated or ozone-treated PET fibers

PET bundles or monofilaments were stretched into the grooves of polypropylene (PP) cards and then fixed with adhesive tape that resists high temperatures (3M®) (Fig. 1). These cards were then inserted into polytetrafluoroethylene (PTFE) moulds ($40\times10\times5$ mm^3) and heated in an oven for 1 h at 80 °C. Afterwards, 1 mL of HEMA reactive solution (bubbled with N_2 for 20 min) containing 0.5 wt% of EGDMA and 0.1 wt% of AIBN, was injected into the mould and the polymerization carried out at 80 °C for 150 min. Finally, the mould was slowly cooled in the closed oven and the samples removed and immersed in bidistilled water. In these conditions, samples with embedded fibers of ca. 10 mm, and with free-fiber length of 20 mm were obtained. In pHEMA hydrogels with PET monofilaments, the composites were sliced to yield an embedded monofilament of ca. 6 mm.

The pull-out tests were performed in a TIRA 2705 apparatus, using a crosshead speed of 5 mm/min and a load-cell of 20 N (samples with monofilaments) or 5 kN (samples with bundles). The wet samples were hold at 2.5 bar in the two extremities and the test was stopped when the monofilaments/bundles were totally removed from the pHEMA hydrogel. The assays were carried out at 22 ± 1 °C and 50 ± 5% of relative humidity.

2.11. Hydrogel swelling measurements

The hydrogels were prepared in PTFE moulds according to the methodology described in the pull-out tests without the PP cards. The gels were subsequently removed from the moulds and immersed in bidistilled water, at 37 °C. At regular intervals, the swollen gels were removed, blotted with filter paper to remove surface water, weighed, and returned to the same container (with fresh bidistilled water) until weight stabilization was observed (W_s; ca. 6 days). The gels were then dried at room temperature, under vacuum, and weighed to determine the dried weight, W_d. The swelling ratio at equilibrium (SRE) was calculated according to Eq. (5)

$$SRE = \frac{W_s - W_d}{W_d} \quad (5)$$

2.12. Statistical analysis

One-way analysis of variance with Bonferroni post-test was performed for statistical tests by using GraphPad Prism 3.0 (San Diego, CA) software package. A p value of <0.05 was considered to be statistically significant.

3. Results and discussion

3.1. Surface chemistry of ozone-treated PET

The surface properties of ozone-treated PET were followed by contact angle measurements, XPS and IRAS/ATR-IR to obtain information about the first 5 Å, 21–81 Å (by the use of Eq. (3) and θ values of 90 and 15°) and 45–5150 Å (by the use of Eq. (4) for ATR studies, and the film thickness for IRAS studies; see below), respectively.

Table 1
Contact angles and O:C atomic ratio of ozone-treated PET films

Ozonation time (h)	Treatment	θ_{static} (°)	$\theta_{advancing}$ (°)	$\theta_{receding}$ (°)	O:C Atomic ratio for different take-off angles[a]		
					90°	15°	30°
0	Unwashed	72.5±2.9	78.4±1.4	51.1±2.1	0.380	0.365	0.349
1		68.1±1.1	74.5±0.8	42.4±1.8	0.389	–	–
3		60.6±0.3	66.0±2.6	36.2±1.1	0.406	0.398	–
6		50.1±1.0	54.1±0.8	20.7±2.5	0.413	0.400	0.388
1	Washed	66.4±0.9	70.3±1.0	44.1±2.4	0.388	0.380	–
3		61.6±1.8	67.7±1.4	36.0±1.8	0.391	0.376	–
6		57.4±1.5	61.9±1.1	23.3±3.2	0.395	0.400	0.394

[a] The depths are ~81, ~41 and ~21 Å, using take-off angles of 90, 30 and 15°.

3.1.1. Contact angle measurements

The ozone treatment of PET was followed by static or dynamic (advancing and receding) water contact angle measurements. The advancing water contact angle is most sensitive to the low-energy (unmodified) components of the surface [21]. The receding contact angle tends to be more sensitive to the high-energy, oxidized groups introduced by the surface treatment [21]. As expected, the wettability of PET surface increases as a function of ozonation time, as shown by the decrease in static, advancing and receding contact angles (Table 1). This shows the formation of polar groups at the surface of PET. Changes in contact angle brought about by ozonation are partially reversed by washing with water (Table 1). The resulting increase in the measured contact angle (observed for PET treated by ozone for 3 and 6 h) is attributable to the removal of oxidized polymers (OP) that were formed during ozonation [7,8] (see below).

3.1.2. XPS analysis

According to the results obtained by XPS (Table 1), the incorporation of oxygen into PET (given by O:C) increases as a function of ozonation time. This effect is very slow, being the ΔO:C (difference between the O:C of the ozone-treated PET and the O:C of untreated PET) of 0.03–0.04 after 6 h of reaction. The incorporation of oxygen into PET was also studied at different depths, by using different take-off angles (90, 30 and 15° corresponding to analysis depths of ∼81, ∼41 and ∼21 Å, respectively). According to Table 1, the O:C values increase from the surface to the interior of the film. However, care must be taken in the interpretation of the data since the untreated PET film presents a low O:C for the outermost surface (the percentages of carbon and oxygen were 74.15 and 25.85, respectively, and thus suggesting a carbon contamination). Therefore, if the O:C of ozone-treated film is subtracted from the O:C of the untreated film at the same take-off angle, the resulting ΔO:C is higher for lower take-off angles.

The O:C ratio for washed PET films was also determined by XPS (Table 1). Hill et al. [8] founded by XPS (at a depth of 48.7 Å) that washing ozone-treated PET films with water decreased the ΔO:C ratio by ca. 30%, however, the relationship between the removal of OP and sampling depth was not reported. In this work, the O:C values decreased after the washing procedure and thus confirming the removal of OP. This effect was variable according to the sampling depth and ozonation time. For example, PET exposed to ozone for 6 h and then washed, the decrease in the ΔO:C ratio is ∼54% at a depth of 81 Å and null at depths of 41 and 21 Å. However, a different pattern was found for PET exposed to ozone for 3 h, where the removal of OP at higher depths was less efficient than at the outermost surface.

Functional groups at the surface of untreated and ozone-treated PET were also characterized by XPS. On the as-received sample, the experimental concentrations of carbon and oxygen measured from the C1s and O1s spectral areas were 72.5% and 27.5% (spectrum obtained using a take-off angle of 90°), respectively, and thus were close to the values expected for this polymer (71.5% C and 28.5% O; Fig. 2(A)). The high-resolution C1s and O1s core-level photoemission spectra of the as-received PET are shown in

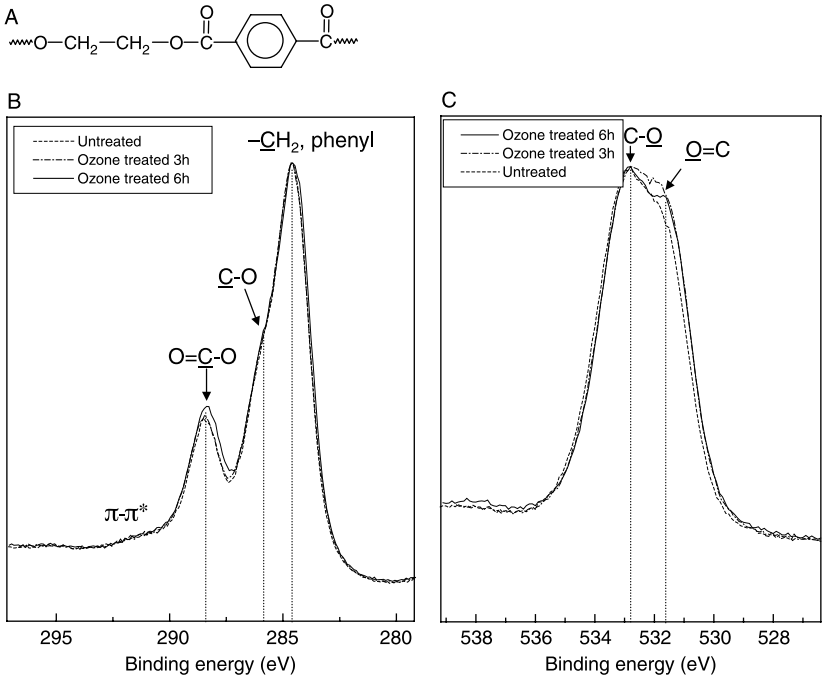

Fig. 2. (A) Schematic representation of PET. (B), (C) C1s and O1s XPS high resolution spectra of ozone-treated PET films for different times. The spectra were normalized taking into account the peaks at 284.6 eV (C1s spectra) and 533.1 eV (O1s spectra). A take-off angle of 90° was used for all the samples.

Fig. 2(B) and (C), respectively. The primary components of C1s spectrum correspond to the carbon atoms of the phenyl ring (284.6 eV, FMHM = 1.74), methylene carbon atoms singly bonded to oxygen C–O (286.1 eV, FMHW = 1.57) and to the ester carbons O–C=O (288.6 eV, FMHM = 1.72) [5]. Finally, the low-intensity peak at 291.2 eV, which occurs in polymers containing conjugated electrons, is assigned to a π–π* transition [5]. On the other hand, the O1s signal of PET is characterized by a doublet peak corresponding to the singly-bound (533.1 eV) and doubly-bound oxygen (531.5 eV) species as well by a low intensity satellite peak at 538.0 eV assigned to the shake-up satellite structure.

Some information that concerns the nature of the functional groups introduced by ozone treatment can be determined from the C1s spectra (Fig. 2(B)). In this spectra normalized taking into account the aromatic peak at 284.6 eV, the intensity of the peak corresponding to the carbon in O–C=O group increases as a function of ozonation time, while the intensity of the peak assigned to carbon in C–O group remained practically unchanged. The increase and broadening of the O–C=O peak is indicative of the formation of carboxylic and carbonyl groups [6,22,23]. Carboxylic groups are formed due to chain scission of the polymer backbone while carbonyl groups (most likely belonging to anhydride functionalities since aldehyde groups are rapidly attacked by ozone to give carboxyl groups [24]) are likely formed by oxygen incorporation. The deconvolution of the C1s spectra for ozone-treated PET film for 6 h shows that carbonyls (286.8 eV) and carboxyl groups (289.4 eV) account for ca. 1.2 and 1.8% of the carbon atoms (analysis depth of ~81 Å), respectively, whereas in the corresponding washed film the carbonyls and carboxyl groups account for 1.1 and 0.3%, respectively.

The presence of carboxylic and hydroxyl groups in ozone-treated PET for 6 h (unwashed) was also confirmed by a labelling procedure involving 1,1′-carbonyldiimidazole and heptafluorobutyryl chloride [12], respectively, and further characterization by XPS. The content of carboxylic and hydroxyl groups at an analysis depth of ~81 Å was 0.12 and 0.03% of the carbon atoms, respectively. In the untreated PET, no carboxylic groups were detected while hydroxyl groups accounted for 0.13% of the carbon atoms. The lower content of hydroxyl groups in ozone-treated PET as compared to the untreated sample indicates that some of the original hydroxyl groups did react with ozone. In fact it has been reported that alcohols are very reactive with ozone yielding carbonyl groups [24]. On the other hand, the content of carboxyl was lower than the one calculated by deconvolution of the C1s spectra even in the case, where the sample was washed with water. The error associated with the deconvolution procedure as well as the use of polar organic solvents in the labelling process [12], which may extract components out the samples, may contribute for the differences found.

3.1.3. IRAS and ATR-IR analysis

Fig. 3 displays the IRAS spectra of untreated and ozone-treated PET sample for 6 h. A major difference between the IRAS spectra of untreated and ozone-treated PET is related to the ratio between the bands at 1738 ($\nu_{C=O}$) (region from 1800 to 1650 cm^{-1}) and 1410 ($\nu_{=C-H,aromatic}$) cm^{-1} [25,26]. According to Table 2, this ratio is higher in case of ozone-treated PET than on untreated one and thus showing that the ozonation process increased the –C=O groups content in PET. As expected, this ratio increases as a function of ozonation time (Table 2). According to Table 3, in general, the ratio A_{1738}/A_{1410} decreased with the increasing in sampling depth. Assuming a linear regression between these two variables, the results show that the ozonation process affected PET surface upon ca. 0.9 μm in depth.

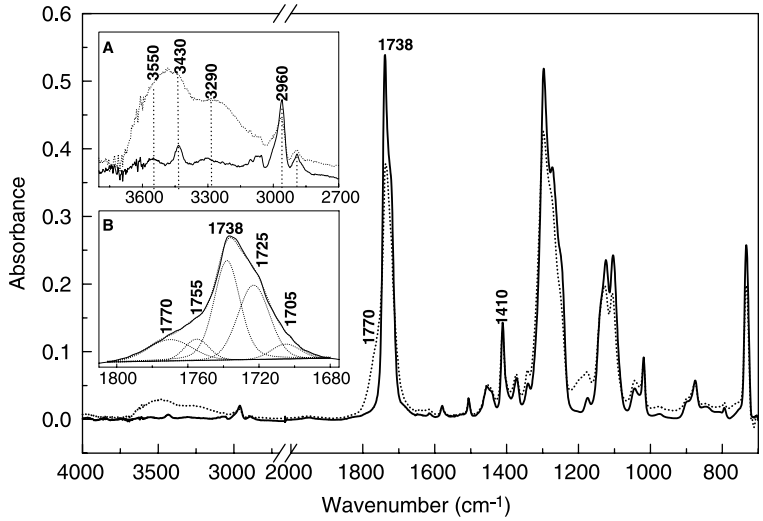

Fig. 3. IRAS spectra of untreated (full) and ozone-treated PET film for 6 h (dotted). The spectra were obtained from PET deposited on gold plates at a thickness of 330 nm. (A) Magnification of the region between 3800 and 2700 cm^{-1}. (B) Curve-fitted –C=O stretching region of PET film exposed to ozone for 6 h.

Table 2
Variation of normalized –C=O and COOH absorptions for ozone-treated PET films, as measured by IRAS

Ozonation time (h)	$(A_{1738}/A_{1410})_{ozonated}/(A_{1738}/A_{1410})_{untreated}$		$(A_{3290}/A_{2960})_{ozonated}/(A_{3290}/A_{2960})_{untreated}$	
	Unwashed films	Washed films	Unwashed films	Washed films
1	1.088	1.083	4.491	1.747
3	1.170	1.128	6.838	2.407
6	1.295	1.212	6.571	3.554

The thickness of PET film deposited onto gold plates was ca. 330 nm, as measured by ellipsometry.

In ozone-treated PET film, the broad band with maximum at 1738 cm^{-1} (Fig. 3) suggests a contribution of several components at 1770, 1755, 1738, 1725 and 1705 cm^{-1}. Since the intrinsic intensity of each component is likely different from the others (and thus a peak may be more intense than the others but corresponding to a lower quantity of the specimen) no quantitative comparison should be attempted. The component at 1705 cm^{-1} is likely assigned to the stretching of –C=O in carboxylic groups based in reported infrared spectra of benzoic acid [27] and other related compounds [28]. The two components at 1725 and 1738 cm^{-1} are attributed to the stretching of –C=O moiety in the original ester group, since those were observed in the untreated sample (data not shown). Finally, the components at 1755 and 1770 cm^{-1} are attributed to the vibrations of two –C=O groups in the anhydride groups [27,29].

Changes in the IR spectrum of ozone-treated PET film were also observed in the range of 4000–3000 cm^{-1} (Fig. 3). The peak at 3550 cm^{-1} is assigned to the stretching of terminal hydroxyl groups of PET [10]. This peak overlaps with the peak at 3430 cm^{-1}, attributed to the first overtone of the fundamental C=O absorption [10] and, therefore, making it difficult to draw any conclusion. The peak at 3290 cm^{-1} is assigned to the carboxylic O–H stretching vibration [10] and according to Fig. 3 is more intense on ozone-treated than untreated PET. Table 2 shows the ratio between the areas at 3290 and 2960 cm^{-1} (ν_{C-H}) to allow quantitative comparison between samples exposed to ozone for different times. This ratio increases for the first 3 h and thus showing that an increasing number of carboxyl groups are formed.

Table 3
Variation of normalized –C=O absorption in ozone-treated PET with sampling depth

d_p, nm	$(A_{1738}/A_{1410})_{ozonated}/(A_{1738}/A_{1410})_{untreated}$	
	Unwashed films	Washed films
4.5[a]	1.368	n.d.
17.8[a]	1.375	1.356
110[a]	1.277	1.222
515[b]	1.111	n.d.

n.d., Not determined.

[a] PET solutions at different concentrations (0.36, 0.072 and 0.0144%, w/w) in trifluoroacetic acid were deposited on gold plates by spin coating and treated by ozone for 6 h (see Materials and methods). The thickness of PET film deposited into gold plates was determined by ellipsometry. The values correspond also to the penetration depth of infrared radiation in IRAS.

[b] A PET film (thickness of 56 μm) was exposed to ozone for 6 h and the ATR-IR spectrum acquired afterwards. The penetration depth of the infrared radiation within the PET film was calculated according to Harrick equation (see Materials and methods) for a wavenumber of 1738 cm^{-1}.

Washed PET films were also characterized by IRAS spectroscopy (Table 2). As expected, the washing procedure decreased the ratio A_{1738}/A_{1410} on PET surface due to the removal of OP by the water. Furthermore, considering the variation of the components at 1755 and 1705 cm^{-1}, the washing procedure changed the ratio between the different species (Table 4). The deconvolution of the –C=O stretching region shows that the component at 1705 cm^{-1} (attributed to carboxylic groups) decreased ca. 80% on PET treated with ozone for 1 and 3 h and ca. 40% on PET treated for 6 h. In fact a similar pattern was found for the different samples by the ratio A_{3290}/A_{2960} (Table 2), corresponding also to the content of carboxyl groups that are present on ozone-treated PET. The high decrease in carboxyl groups for the overall samples is likely related to the fact that these groups are formed by scission of the initial polymer backbone and, therefore, are easily removed by water. In contrast, the band at 1755 cm^{-1} (attributed to the anhydride groups) was less affected by the washing procedure (below 15%). These groups are formed by oxygen incorporation and since their removal by washing is comparatively lower than the one observed for carboxyl groups suggests that anhydrides are mainly formed in different polymer chains.

In summary, the results obtained by contact angle measurements, XPS and IRAS/ATR-IR suggest that the ozonation proceeded through oxidation and chain scission, leading to the formation of anhydride, carboxylic and hydroxyl groups. According to earlier studies [24,30] ozone may react with different polymer chains by hydrogen abstraction leading to radical formation. This radical can react with ozone forming a peroxy group, which can lead to the formation of different groups. Ozone-treated PET for 6 h was selected for further characterization due to the relative higher level of surface modification.

Table 4
Results obtained from the deconvolution of –C=O stretching region from ozone-treated PET films at different times before and after a washing step

Ozonation time (h)	Treatment	% of –C=O band		
		1770 cm^{-1}	1755 cm^{-1}	1705 cm^{-1}
1	Unwashed	2.7	3.0	3.7
3		6.4	4.9	5.0
6		12.0	7.8	5.3
1	Washed	3.1	2.9	0.7
3		3.9	5.5	0.7
6		7.1	6.7	3.3

The percentages from the bands at 1738 and 1725 cm^{-1} were not included.

3.2. Morphology of ozone-treated PET films

Tapping mode AFM analysis was undertaken to study the surface morphology of untreated and ozone-treated PET samples. Height and phase images were recorded simultaneously and the results shown in Fig. 4. According to Table 5, the roughness average of ozone-treated PET is higher than the value obtained for the untreated sample. The morphology of ozone-treated PET is clearly different from the one observed in the untreated one. In case of ozone-treated PET film (Fig. 4(C) and (D)), the surface is fully covered either with small (diameter <0.1 μm) or large spherical particles (diameter >0.15 μm). These particles are likely OP formed during the ozonation reaction. A similar phenomenon was observed on PET films treated by corona-discharge [6] and ultraviolet-ozone [31]. In this last case, particles with size of ca. 0.2 μm were observed during ultraviolet-ozone treatment for short period of times (minutes range) and the roughness of the film increased from 1.0 nm (untreated) to ca. 5 nm. In the present work, it is likely that large spherical particles are formed through an agglomeration process involving several small particles, as illustrated by AFM results.

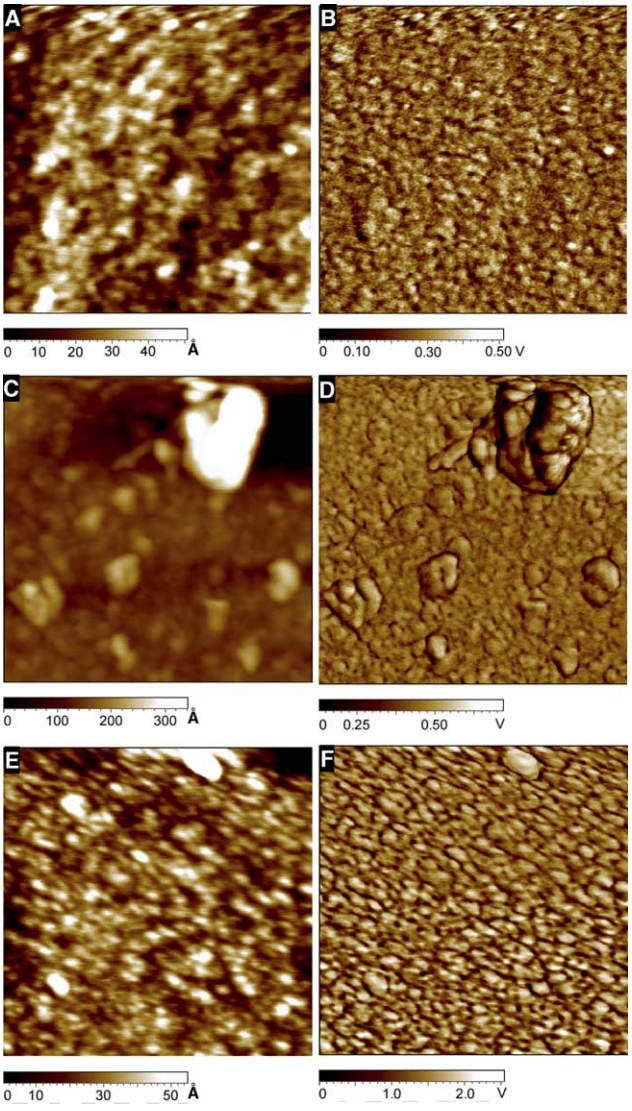

Fig. 4. Tapping mode AFM images (height (left) and phase (right) imaging) from the surfaces of untreated PET (A, B), ozone-treated PET for 6 h (C), (D) and ozone-treated PET for 6 h and washed with water (E), (F). Scan areas of 1×1 μm^2 were used.

AFM results also confirm the removal of OP from the surface (Fig. 4(E) and (F)). After rinsing the ozone-treated PET film with water, the spherical particles formed by OP were almost totally removed. This confirms the results obtained by contact angle measurements, XPS and IRAS/ATR results showing the decrease in polar groups after a washing step. Moreover, the roughness of the sample was reverted to a value found in the untreated one.

3.3. Pull-out tests

Pull-out tests have been used for measuring the interfacial bond strength between PET monofilaments and pHEMA hydrogels and thus yielding an estimation of the adhesion. This test measures the force, F_{max}, required to pull out a fiber whose end is embedded in a matrix. The F_{max} is then converted into the apparent interfacial shear strength, τ_i, according to Eq. (6) [32,33]:

$$\tau_i = \frac{F_{max}}{\pi DL} \tag{6}$$

where F_{max} is the maximum tensile load, and D and L are the fiber diameter and the embedded fiber length, respectively. Experiments with different polymer/fiber systems have demonstrated a linear relationship between τ_i (also called 'practical' adhesion [34]) and the work of adhesion ('fundamental' adhesion [34]).

Three types of PET monofilaments were selected for pull-out tests: untreated, ozone-treated for 6 h and ozone-treated for 6 h and immersed in HEMA reactive solution for 18 h at 4 °C. The reason behind the selection of this last sample was to evaluate whether a possible migration of HEMA solution into the bulk of PET had a positive effect in the τ_i values. pHEMA hydrogels with a thickness of 5 mm and containing one type of PET monofilament were used for the overall set of experiments. These samples were swollen during 7 days in bidistilled water before achieving the equilibrium swelling (SRE of 0.56 ± 0.057).

Typical load-displacement curves obtained by pull-out tests are shown in Fig. 5(A). These curves show that the measured force increases until a maximum and drops after the debonding is completed. Afterwards, the force decreases further and is controlled by the friction between the fiber and polymer. Fig. 5(B) shows the τ_i values obtained for the different samples. The stress to pull out the ozonated monofilament from pHEMA hydrogel is ca. 65% higher than the one obtained for untreated PET monofilament. The high τ_i values found on samples comprising ozone-treated

Table 5
Roughness average (S_a) and root mean square (S_q) of untreated and ozonetreated PET as calculated from AFM results

Sample	S_a (nm)	S_q (nm)
Untreated PET	1.1 ± 0.6^a	1.4 ± 0.7^a
Ozone-treated PET for 6 h	4.2 ± 1.4^b	7.0 ± 2.5^b
Ozone-treated PET for 6 h and washed	0.9 ± 0.1	1.2 ± 0.2

Average ± SD ($n=5$). Scan areas of 1×1 μm^2 were used.
[a] The roughness was statistically different to the one observed in the ozone-treated PET for 6 h ($p<0.001$) but not in ozone-treated PET for 6 h and washed ($p>0.05$).
[b] The roughness was statistically different ($p<0.001$) to the one observed in untreated PET and ozone-treated PET for 6 h and washed.

PET monofilaments show that ozone treatment had a beneficial effect in the adhesion of the polymer into pHEMA hydrogels. This may be due to hydrogen bonds occurring between the polar functionalities of ozone-treated PET (through the –C=O of carboxylic and anhydride groups since they are at the outermost surface according to XPS results) and the hydroxyl groups from pHEMA hydrogel. Evidence for this type of interaction comes from autoadhesion studies in PET [35,36]. It has been reported that two PET films treated by corona discharge adhered strongly to each other under conditions that give no adhesion with untreated film. Chemical and physical tests have shown that the adhesive bond is a hydrogen bond between the hydrogen of a hydroxyl group created by corona in one surface with carbonyl groups in the other surface [35,36].

The results also show that the immersion of ozone-treated PET fibers into HEMA reactive solution before its polymerisation did not increase the adhesion between the fiber and the pHEMA matrix when compared to the values obtained in samples with ozone-treated PET without previous immersion. In fact, the τ_i value calculated was not statistically significant ($p>0.05$) either to the one obtained with ozonated or untreated monofilament. In this last case likely due to the low number of samples tested and

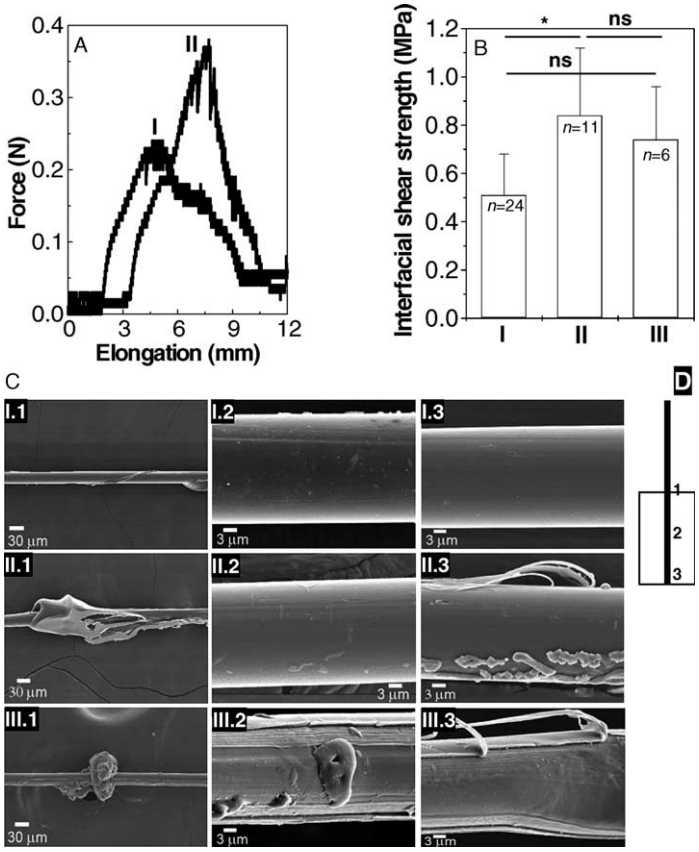

Fig. 5. (A) Typical force-elongation curves obtained during pull-out tests in pHEMA hydrogels containing untreated (I) and ozone-treated PET monofilaments (II). (B) Interfacial shear strength (average ± SD) obtained for pHEMA hydrogels containing PET monofilaments treated in different ways: (I) untreated, (II) treated with ozone for 6 h and (III) treated with ozone for 6 h and immersed in HEMA reactive solution for 18 h (see Materials and methods). (C) SEM micrographs of PET monofilaments after pull-out tests: untreated (I.1; I.2; I.3), ozone-treated for 6 h (II.1; II.2; II.3) and ozone-treated for 6 h and subsequently immersed in HEMA reactive solution for 18 h (III.1; III.2; III.3). (D) Schematic representation of embedded monofilament in pHEMA hydrogel. The numbers 1, 2 and 3 represent the places, where SEM micrographs were taken. *Statistically significant ($p<0.001$); ns = not statistically significant ($p>0.05$).

consequently to the higher standard deviation obtained (see below).

There are three modes of failure when a fiber is pulled-out from a matrix: adhesive failure at the interface, cohesive failure of the matrix close to the interface and cohesive failure of the fiber close to the interface [33]. After pull-out tests have been performed, the system PET fiber/pHEMA hydrogel was analysed by SEM to evaluate the failure mode. SEM observations of the untreated PET monofilament revealed that in most cases the monofilament surface was very smooth, as shown in Fig. 5(C). In case of ozone-treated PET monofilaments, with or without further treatment, the monofilaments present a 'cone' in the place, where they go through the hydrogel. This 'cone' is part of the hydrogel that was pulled out during the test. Similar cone-like structures have been observed in other composite materials [32,33]. Below the cone structure, the surface of ozone-treated PET monofilaments was either smooth or presented in some regions pHEMA hydrogel attached to it. Taking into account the overall SEM results, the failure took place mainly at the interface and in some cases in the matrix very close to it.

The adhesion between PET bundles and swollen pHEMA hydrogels was also evaluated by pull-out tests. Intervertebral discs of pHEMA hydrogels will be reinforced with PET multi-fibers (bundle) and, therefore, this system would better resemble the real situation. Furthermore, some authors have demonstrated by modelling that interfacial properties in a multi-fiber system deviate from those observed on a single-fiber one [37].

Typical load-displacement curves obtained by pull-out tests of PET bundles immersed into pHEMA hydrogels are shown in Fig. 6(A). These curves comprise the same stages as described previously for the system monofilament/pHEMA hydrogel. In the end of the test (Fig. 6(B)), pHEMA hydrogel attached to PET bundles was observed (no correlation was observed between the content of material attached to PET bundles and their treatment). This shows that the failure in the fiber pull-out did not take place at the interface fiber/matrix but at the bulk matrix and thus preventing the determination of interfacial shear strength. However, according to Fig. 6(C), the force necessary to provoke the failure of the bulk hydrogel matrix is different for each condition, and shows the same pattern observed for the monofilament pull-out tests. The force to pull-out the ozone-treated PET bundle (similar results were obtained for the ozone-treated PET bundle with immersion on HEMA reactive solution) from pHEMA hydrogel is ca. 81% higher than the one observed for the untreated bundle. The higher value observed on this last system is likely related to the higher adhesion between PET bundle and pHEMA hydrogel. According to a model recently

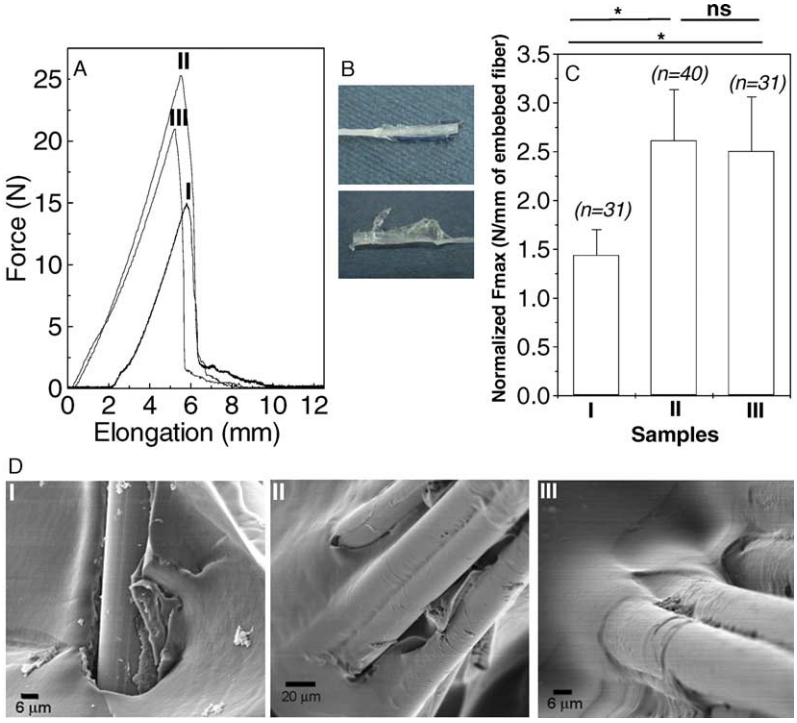

Fig. 6. (A) Typical force-elongation curves obtained during pull-out tests in pHEMA hydrogels containing PET bundles that were untreated (I), treated with ozone for 6 h (II), and treated with ozone for 6 h and immersed in HEMA reactive solution for 18 h (III). (B) Photographs of PET bundles after pull-out test. (C) Normalized maximum force (average ± SD) to pull-out the embedded bundle in pHEMA hydrogels. (I) Untreated, (II) treated with ozone for 6 h and (III) treated with ozone for 6 h and immersed in HEMA reactive solution for 18 h (see Materials and methods). (D) SEM micrographs of PET bundles after pull-out tests: untreated (I), ozone-treated for 6 h (II) and ozonetreated PET bundles immersed in HEMA reactive solution for 18 h (III). * Statistically significant ($p < 0.001$); ns = not statistically significant ($p > 0.05$).

developed [37], the stress transfer in a multi-fiber composite involves several components. When an external stress is applied on the fiber, stress transfers from the fiber to the matrix in its vicinity and, in turn, to the 'composite medium' (in this case bulk hydrogel) via the interface shear stresses. We speculate that when the adhesion between the fiber and the matrix is poor, the shear stress is not uniformly distributed along the embedded fiber length and, therefore, failure of the bulk matrix is highly favoured than when a good adhesion is observed.

SEM also confirms the superior adhesion of ozone-treated PET bundles, with or without further treatment, with pHEMA hydrogels (Fig. 6(D)). In the ozone-treated PET bundles (with or without further treatment), the pHEMA hydrogel coated entirely the surface of PET fibers and no discontinuity between both materials was observed. In case of untreated PET bundle, there was a discontinuity between PET and pHEMA hydrogel, showing that the adhesion between both materials was poor.

4. Conclusions

The ozonation reaction of PET proceeded through chain scission and oxygen incorporation. Different functionalities can be observed after ozone-treatment of PET including carboxylic, anhydride and hydroxyl groups. Following a washing step the content of polar groups decreases due to the removal of oxidized polymers. At the outermost surface, this was characterized by the removal of spherical particles. The decrease in oxidized polymers was not higher than 67% at sampling depths between 15 and 81 Å and 28% at sampling depths upon 0.33 μm. In addition, the ratio between the functional groups changes being carboxylic groups easily removed while anhydrides more firmly attached. The polar groups introduced by ozone on PET enhanced the adhesion between PET fibers and pHEMA hydrogels. According to pull-out tests, the apparent interfacial shear strength is 65% higher on pHEMA hydrogel containing an ozonated than an untreated PET monofilament. In addition, the force to pull-out an ozone-treated PET bundle (similar results were obtained for the ozone-treated PET bundle with immersion on HEMA reactive solution) from pHEMA hydrogel is ca. 81% higher than the one observed for the untreated bundle.

Acknowledgements

We are grateful for the financial support of the European agency through the project DISC G5RD-CT-2000-00267. We would like to thank Manuela Brás and Isabel Amaral for the assistance with AFM analyses and Prof Luigi Ambrosio and Dr Filippo Causa from University of Naples for the PET samples used in this work and their characterization.

References

[1] Hart BL, Deyo RA, Cherkin DC. Spine 1995;20:11–19.
[2] Bao Q-B, McCullen GM, Higham PA, Dumbleton JH, Yuan HA. Biomaterials 1996;17:1157–67.
[3] Martz EO, Goel VK, Pope MH, Park JB. J Biomed Mater Res (Appl Biomater) 1997;38:267–88.
[4] Strobel M, Walzak MJ, Hill JM, Lin A, Karbashewski E, Lyons CS. J Adhes Sci Technol 1995;9(3):365–83.
[5] Le QT, Pireaux JJ, Caudano R. J Adhes Sci Technol 1997;11:735–51.
[6] O'Hare L-A, Smith JA, Leadley SR, Parbhoo B, Goodwin AJ, Watts JF. Surf Interface Anal 2002;33:617–25.
[7] Walzak MJ, Flynn S, Foerch R, Hil JM, Karbashewski E, Lin A, et al. J Adhes Sci Technol 1995;9:1229–48.
[8] Hill JM, Karbashewski E, Lin A, Strobel M, Walzak MJ. J Adhes Sci Technol 1995;9(12):1575–91.
[9] Blais P, Day M, Wiles DM. J Appl Polym Sci 1973;17:1895–907.
[10] Day M, Wiles DM. J Appl Polym Sci 1972;16:175–89.
[11] Nissen KE, Stevens MG, Stuart BH, Baker AT. J Polym Sci, Part B: Polym Phys 2001;39:623–33.
[12] Chen W, McCarthy TJ. Macromolecules 1998;31:3648–55.
[13] Mougenot P, Marchand-Brynaert J. Macromolecules 1996;29: 3552–9.
[14] Hebeish A, Shalaby SE, Bayazeed AM. J Appl Polym Sci 1981;26: 3253–69.
[15] Degert C, Dupuy B, Labat B, Baquey C. Biomat Art Cells Immobil Biotech 1993;21:553–61.
[16] Ambrosio L, Netti PA, Iannace S, Huang SJ, Nicolais L. J Mater Sci: Mater Int Med 1996;7:251–4.
[17] Rule M. Physical constants of poly(oxyethylene-oxyterephthaloyl) (poly(ethylene terephthalate)). In: Brandrup J, Immergut EH, Grulke EA, editors. Polymer handbook. New York: Wiley; 1999. p. V/113–V/118.
[18] Seah MP, Dench WA. Surf Interface Anal 1979;1:2–11.
[19] Strobel M, Lyons C, Strobel JM, Kapaun RS. J Adhes Sci Technol 1992;6(4):429–43.
[20] Harrick NJ. Internal reflection spectroscopy. 2nd ed. New York: Wiley; 1979.
[21] Andrade JD, Smith LM, Gregonis DE. The contact angle and interface energetics. New York: Plenum press; 1985. p. 249–92.
[22] Peeling J, Clark DT. J Polym Sci: Polym Chem Ed 1983;21:2047–55.
[23] Peeling J, Courval G, Jazzar MS. J Polym Sci: Polym Chem Ed 1984; 22:419–28.
[24] Razumovskii SD, Kefeli AA, Zaikov GE. Eur Polym J 1971;7: 275–85.
[25] Wang Y, Lehmann S. Appl Spectrosc 1999;53:914–8.
[26] Liang CY, Krimm S. J Mol Spectrosc 1959;3:554–74.
[27] Pavia DL, Lampman GM, Kriz GS. Introduction to spectroscopy. 2nd ed. New York: Harcourt Brace College Publishers; 1996. p. 14–95.
[28] Carlsson DJ, Wiles DM. Macromolecules 1969;2(6):597–606.
[29] Socrates G. Infrared and Raman characteristic group frequencies: Tables and charts. 3rd ed. New York: Wiley; 2001. p. 115–56.
[30] Rabek JF, Lucki J, Rånby Y, Watanabe Y, Qu BJ. Photoozination of polypropylene. Washington, DC: American Chemical Society; 1988. p. 187–200.
[31] Ton-That C, Teare DOH, Campbell PA, Bradley RH. Surf Sci 1999; 433–435:278–82.
[32] Tanaka K, Minoshima K, Grela W, Komai K. Compos Sci Technol 2002;62:2169–77.
[33] Sadiku ER, Sanderson RD. Macromol Mater Eng 2001;286:535–45.
[34] Pisanova E, Zhandarov S. J Adhes 2001;75:89–127.
[35] Owens DK. J Appl Polym Sci 1975;19:3315–26.
[36] Briggs D, Rance DG, Kendall CR, Blythe AR. Polymer 1980;21: 895–900.
[37] Fu S-Y, Yue C-Y, Hu X, Mai Y-W. Compos Sci Technol 2000;60: 569–79.